DRAFT VERSION DECEMBER 20, 2018
Typeset using LaTeX **twocolumn** style in AASTeX62

Supplement to: Electron energy partition across interplanetary shocks

LYNN B. WILSON III[1] AND *et al.*[2]

[1] *NASA Goddard Space Flight Center, Heliophysics Science Division, Greenbelt, Maryland, USA.*
[2] *Important Place with Important People, Important City, Important State/Province, Important Country.*

(Received December 20, 2018; Revised Month DD, YYYY; Accepted N/A)

Submitted to ApJ

ABSTRACT

This is supplemental material to the multi-part papers entitled, "Electron energy partition across interplanetary shocks"

Keywords: plasmas — shock waves — (Sun:) solar wind — Sun: coronal mass ejections (CMEs)

1. PARAMETERS AND SHOCK ANALYSIS

We use the following notations for any quantity, Q, thoughout this paper: Q_o, δQ, and $\langle Q \rangle_j$, where Q_o is any quasi-static quantity, δQ is any fluctuating or high pass filtered quantity, $\Delta Q = \langle Q \rangle_{dn}$ - $\langle Q \rangle_{up}$, and $\langle Q \rangle_j$ is the time average of any quantity over region j = upstream (up) or downstream (dn). Note that Q_o is not the same as $\langle Q \rangle_j$ in this context.

Herein we use the following parameter definitions: $\mathbf{B}_o$ is the quasi-static magnetic field vector [nT]; $\mathbf{V}_{bulk}$ is the bulk flow velocity vector [$km\ s^{-1}$]; n_s is the number density of species s [cm^{-3}]; m_s is the mass of species s [kg]; T_s is the scalar temperature of species s [eV]; $W_s = \sqrt{k_B\ T_s / m_s}$ is the rms thermal speed of species s; $V_A = B_o / \sqrt{\mu_o\ m_i\ n_i}$ is the Alfvén speed [$km\ s^{-1}$]; $\delta\mathbf{B}$ is the high pass filtered fluctuating magnetic field due to a whistler precursor [nT]; $\Delta|\mathbf{B}_o|$ is the change in the magnetic field magnitude across a shock ramp [nT]; SCF is the spacecraft rest frame; and SHF is the shock rest frame.

All shock parameters used herein were taken from the Harvard Smithsonian Center for Astrophysics' Wind shock database (WSDB), which can be found at: https://www.cfa.harvard.edu/shocks/wi_data/. The WSDB provides tables of numerical solutions to the Rankine-Hugoniot relations (e.g., Koval & Szabo 2008; Szabo 1994; Vinas & Scudder 1986) for eight different methods (see Section 1.1 for definitions). The first table, titled *General Information*, on each event webpage lists the selected best method from which we take the values for all events examined herein (e.g., second column of Table 1).

In the tables that follow on each event webpage of WSDB, some parameters are listed by name while others use symbols or abbreviations. In the following we will state our definition followed by the WSDB equivalent label in parentheses and italicized text. Rather than repeated state that $\langle Q \rangle_j$ corresponds to the quantity Q averaged over the j^{th} region, we will simply imply it for brevity. These parameters we used are: $\langle W_s \rangle_j (Ws)$ is the rms thermal speed of species s [$km\ s^{-1}$]; $\langle V_A \rangle_j (Alfven\ Speed)$ is the Alfvén speed averaged [$km\ s^{-1}$]; $\langle C_s \rangle_j (Sound\ Speed)$ is the sound or ion-acoustic sound speed, defined here as $\sqrt{\frac{5}{3}}\ \langle W_i \rangle_j$; $\langle \beta_{Tot} \rangle_j (Plasma\ Beta)$ is the "total" plasma beta, define here as $(3/5) C_s{}^2 / V_A{}^2$; $\hat{\mathbf{n}}$(*Nx*, *Ny*, and *Nz*) is the shock normal unit vector [GSE]; $\mathcal{R}(Compression)$ is the shock density compression ratio, defined as $\langle n_i \rangle_{down} / \langle n_i \rangle_{up}$; $\langle \theta_{Bn} \rangle_{up} (ThetaBn)$ is the shock normal angle, defined as the acute reference angle between $\langle \mathbf{B}_o \rangle_{up}$ and $\hat{\mathbf{n}}$; $|V_{shn}| (Shock\ Speed)$ is the upstream shock normal speed in the SCF (determined numerically from Equation 4d); $\langle U_{shn} \rangle_j (dV)$ flow speed along shock normal in the SHF [$km\ s^{-1}$] (defined in Equation 7); $\langle M_A \rangle_j$(not shown) is the Alfvénic Mach number, defined as $\langle |U_{shn}| \rangle_j / \langle V_A \rangle_j$; and $\langle M_f \rangle_j (Fast\ Mach)$ is the fast mode Mach number,

Corresponding author: L.B. Wilson III
lynn.b.wilsoniii@gmail.com

defined as $\langle |U_{shn}| \rangle_j / \langle V_f \rangle_j$ where V_f is the MHD fast mode phase speed given by:

$$
\begin{aligned}
2 V_f{}^2 &= \left(C_s{}^2 + V_A{}^2 \right) + \\
&\quad \sqrt{\left(C_s{}^2 - V_A{}^2 \right)^2 + 4 C_s{}^2 V_A{}^2 \sin^2 \theta_{Bn}} \qquad (1a) \\
&= \left(C_s{}^2 + V_A{}^2 \right) + \\
&\quad \sqrt{\left(C_s{}^2 + V_A{}^2 \right)^2 - 4 C_s{}^2 V_A{}^2 \cos^2 \theta_{Bn}} \qquad (1b)
\end{aligned}
$$

where C_s is the sound speed (e.g., see Equation 1.9.1 in Krall & Trivelpiece 1973), which is formally defined as:

$$
C_s{}^2 \equiv \frac{\partial P}{\partial \rho_m} \tag{2a}
$$

which is often approximated by assuming an adiabatic equation of state to give:

$$
= \frac{\gamma P}{\rho_m} \tag{2b}
$$

and in a plasma where the ions and electrons carry different polytrope indices, we have the ion-acoustic sound speed:

$$
C_s{}^2 = \frac{k_B \left(Z_i \gamma_e T_e + \gamma_i T_i \right)}{M_i + m_e} \tag{2c}
$$

where k_B = Boltzmann constant, Z_i = ion charge state, and one generally assumes that either $\gamma_e = 1$ (isothermal) and $\gamma_i = 2$ or 3, or $T_e \gg T_i$ and $\gamma_e = 1$ such that $C_s{}^2 \sim \frac{k_B T_e}{M_i}$.

The sound speed reported on the WSDB is, as stated above, give by $\langle C_s \rangle_j = \sqrt{\frac{5}{3}} \langle W_i \rangle_j$, the total plasma beta relies only upon ion data.

1.1. *Conservation Relations*

In the case of a planar shock, we can define the conservation relations called the Rankine-Hugoniot relations across the shock ramp. If we define $\Delta[X]$ = $\langle X \rangle_{dn}$ - $\langle X \rangle_{up}$, where the subscript u(d) corresponds to upstream(downstream). Then we have the following Rankine-Hugoniot relations (Koval & Szabo 2008; Szabo 1994; Vinas & Scudder 1986):

$$
\begin{aligned}
\Delta \left[G_n \right] &\equiv \Delta \left[\rho \left(V_n - V_{shn} \right) \right] = 0 && (3a) \\
\Delta \left[B_n \right] &\equiv \Delta \left[\hat{\mathbf{n}} \cdot \mathbf{B} \right] = 0 && (3b) \\
\Delta \left[\mathbf{S}_t \right] &\equiv \Delta \left[\rho \left(V_n - V_{shn} \right) \mathbf{V}_t - \frac{B_n}{\mu_o} \mathbf{B}_t \right] = 0 && (3c) \\
\Delta \left[\mathbf{E}_t \right] &\equiv \Delta \left[\left(\hat{\mathbf{n}} \times \mathbf{V}_t \right) B_n - \right. \\
&\quad \left. \left(V_n - V_{shn} \right) \left(\hat{\mathbf{n}} \times \mathbf{B}_t \right) \right] = 0 && (3d) \\
\Delta \left[S_n \right] &\equiv \Delta \left[P + \frac{\mathbf{B}_t \cdot \mathbf{B}_t}{2 \ \mu_o} + \rho \left(V_n - V_{shn} \right)^2 \right] = 0 && (3e) \\
\Delta \left[\varepsilon \right] &\equiv \Delta \left[\rho \left(V_n - V_{shn} \right) \left\{ \frac{1}{2} \left(\mathbf{V}_{sw} - V_{shn} \ \hat{\mathbf{n}} \right)^2 \right. \right. \\
&\quad \left. + \frac{\gamma}{\gamma - 1} \frac{P}{\rho} + \frac{\mathbf{B} \cdot \mathbf{B}}{\rho \ \mu_o} \right\} && (3f) \\
&\quad \left. - \frac{B_n \left(\mathbf{V}_{sw} - V_{shn} \ \hat{\mathbf{n}} \right) \cdot \mathbf{B}}{\mu_o} \right] = 0
\end{aligned}
$$

where we have defined:

$$
\begin{aligned}
Q_n &= \mathbf{Q} \cdot \hat{\mathbf{n}} && (4a) \\
\mathbf{Q}_t &= \left(\hat{\mathbf{n}} \times \mathbf{Q} \right) \times \hat{\mathbf{n}} && (4b) \\
&= \mathbf{Q} \cdot \left(\mathbb{I} - \hat{\mathbf{n}} \hat{\mathbf{n}} \right) && (4c) \\
V_{shn} &= \frac{\Delta \left[\rho \ \mathbf{V}_{sw} \right]}{\Delta \left[\rho \right]} \cdot \hat{\mathbf{n}} && (4d)
\end{aligned}
$$

and ρ is the mass density, P is scalar total (ion plus electron) thermal pressure, and γ is the ratio of specific heats or polytrope index. We note that P = $\hat{\mathbf{n}} \cdot \mathbb{P} \cdot \hat{\mathbf{n}}$ = 1/3 Tr[$\mathbb{P}$] $\sim n_o \ k_B \ (T_e + T_i)$ for an ideal gas.

The Harvard Smithsonian Center for Astrophysics' Wind shock database (WSDB), which can be found at: https://www.cfa.harvard.edu/shocks/wi_data/ provides tables of numerical solutions to the Rankine-Hugoniot relations (e.g., Koval & Szabo 2008; Szabo 1994; Vinas & Scudder 1986) for eight different methods, where the labels are defined as:

1. **MC:** Magnetic Coplanarity (e.g., Abraham-Shrauner & Yun 1976; Russell et al. 1983; Vinas & Scudder 1986);
2. **VC:** Velocity Coplanarity (e.g., Abraham-Shrauner & Yun 1976; Russell et al. 1983; Vinas & Scudder 1986);
3. **MX1:** Mixed Mode Normal 1 (e.g., Abraham-Shrauner & Yun 1976; Russell et al. 1983);
4. **MX2:** Mixed Mode Normal 2 (e.g., Abraham-Shrauner & Yun 1976; Russell et al. 1983);
5. **MX3:** Mixed Mode Normal 3 (e.g., Abraham-Shrauner & Yun 1976; Russell et al. 1983);

6. **RH08:** Rankine-Hugoniot with 8 Equations (e.g., Abraham-Shrauner & Yun 1976; Koval & Szabo 2008; Russell et al. 1983; Szabo 1994; Vinas & Scudder 1986);
7. **RH09:** Rankine-Hugoniot with 9 Equations (e.g., Abraham-Shrauner & Yun 1976; Koval & Szabo 2008; Russell et al. 1983; Szabo 1994; Vinas & Scudder 1986); and
8. **RH10:** Rankine-Hugoniot with 10 Equations (e.g., Abraham-Shrauner & Yun 1976; Koval & Szabo 2008; Russell et al. 1983; Szabo 1994; Vinas & Scudder 1986).

The shock normals for the first five methods are given by:

Magnetic Coplanarity (MC)

$$\hat{\mathbf{n}} = \pm \frac{(\langle \mathbf{B}_o \rangle_{up} \times \langle \mathbf{B}_o \rangle_{dn}) \times (-\Delta \mathbf{B}_o)}{|(\langle \mathbf{B}_o \rangle_{up} \times \langle \mathbf{B}_o \rangle_{dn}) \times (-\Delta \mathbf{B}_o)|} \tag{5a}$$

Velocity Coplanarity (VC)

$$\hat{\mathbf{n}} = \pm \frac{\Delta \mathbf{V}_{bulk}}{|\Delta \mathbf{V}_{bulk}|} \tag{5b}$$

Mixed Mode Normal 1 (MX1)

$$\hat{\mathbf{n}} = \pm \frac{(\Delta \mathbf{V}_{bulk} \times \langle \mathbf{B}_o \rangle_{up}) \times \Delta \mathbf{B}_o}{|(\Delta \mathbf{V}_{bulk} \times \langle \mathbf{B}_o \rangle_{up}) \times \Delta \mathbf{B}_o|} \tag{5c}$$

Mixed Mode Normal 2 (MX2)

$$\hat{\mathbf{n}} = \pm \frac{(\Delta \mathbf{V}_{bulk} \times \langle \mathbf{B}_o \rangle_{dn}) \times \Delta \mathbf{B}_o}{|(\Delta \mathbf{V}_{bulk} \times \langle \mathbf{B}_o \rangle_{dn}) \times \Delta \mathbf{B}_o|} \tag{5d}$$

Mixed Mode Normal 3 (MX3)

$$\hat{\mathbf{n}} = \pm \frac{-\Delta \mathbf{B}_o \times (\Delta \mathbf{V}_{bulk} \times \Delta \mathbf{B}_o)}{|\Delta \mathbf{B}_o \times (\Delta \mathbf{V}_{bulk} \times \Delta \mathbf{B}_o)|} \tag{5e}$$

1.2. *Field Transformations*

We can define the velocity transformation from any arbitrary frame of reference (*e.g.* spacecraft frame) to he shock frame of reference as:

$$\mathbf{V}_{sh}{}^{rest} = \mathbf{V}^{arb.} - \left(\mathbf{V}_{sh}{}^{arb.} \cdot \hat{\mathbf{n}} \right) \hat{\mathbf{n}} \tag{6}$$

where $\hat{\mathbf{n}}$ is the vector normal to the assumed planar shock front (see Appendix 1.1). For an experimentalist's purposes, $\mathbf{V}^{arb.} \rightarrow \mathbf{V}_{sw}{}^{SCF}$, where $\mathbf{V}_{sw}{}^{SCF}$ is the bulk flow velocity (e.g., solar wind velocity) in the spacecraft frame (SCF) of reference. Therefore, let us define V_{shn} as the shock normal speed in the SCF and $\langle U_{shn} \rangle_j$ as the flow speed along shock normal in the shock rest frame (SHF) averaged over the j^{th} region. Therefore, Equation 6 goes to:

$$\langle U_{shn} \rangle_j = \left[\langle \mathbf{V}_{sw}{}^{SCF} \rangle_j - (V_{shn}\ \hat{\mathbf{n}}) \right] \cdot \hat{\mathbf{n}} \ . \tag{7}$$

For many applications, one may want to know the upstream incident bulk flow speed in the shock frame, which is given by:

$$\mathbf{V}_u{}^{SHF} = \mathbf{V}_{sw} - (V_{shn}\ \hat{\mathbf{n}}) \ . \tag{8}$$

2. SHOCK PARAMETER TABLES

Table 1. IP Shock Parameters

Ramp Time [UTC]	RH [a] Meth.	$\langle \lvert V_{shn} \rvert \rangle_{up}$ [b] [km/s]	$\langle n_i \rangle_{up}$ [c] [cm^{-3}]	$\langle \lvert \mathbf{B}_o \rvert \rangle_{up}$ [d] [nT]	$\langle M_A \rangle_{up}$ [e]	$\langle M_{cs} \rangle_{up}$ [f]	$\langle M_f \rangle_{up}$ [g]
1995-02-26/02:55:41.125	RH08	285.90± 4.60	21.3±0.70	8.62±8.66	1.43±0.03	2.54± 0.06	1.35±0.03
1995-07-24/02:23:13.000	RH08	375.20± 6.20	8.80±0.20	1.91±1.96	6.24±0.37	4.41± 0.19	4.00±0.15
1995-08-17/02:47:21.925	RH08	463.90± 4.80	2.50±0.20	2.00±2.31	2.50±0.20	2.07± 0.14	1.74±0.10
1995-08-22/12:56:49.250	RH08	381.00± 5.30	3.40±0.20	2.11±2.17	2.57±0.13	2.47± 0.16	1.82±0.04
1995-12-24/05:57:35.375	RH08	422.80± 11.50	16.4±1.50	6.33±6.52	2.95±0.26	4.30± 0.23	2.52±0.17
1996-02-06/19:14:23.700	RH08	383.40± 5.90	7.60±0.30	3.88±4.25	1.71±0.10	2.06± 0.07	1.40±0.06
1996-04-02/10:07:57.525	RH09	155.20± 5.70	12.1±0.30	2.55±2.77	2.29±0.19	1.51± 0.05	1.27±0.07
1996-04-03/09:47:17.152	RH08	379.20± 3.80	14.5±0.50	4.24±4.26	2.02±0.06	2.52± 0.07	1.59±0.02
1996-04-08/02:41:09.765	RH08	182.30± 4.00	15.8±0.20	5.69±5.85	2.42±0.04	3.89± 0.06	2.08±0.03
1997-02-09/12:50:21.125	RH08	635.90± 12.50	3.90±0.20	3.38±3.63	3.14±0.16	2.09± 0.09	1.86±0.06
1997-02-27/17:29:09.087	RH08	557.40± 30.20	1.80±0.10	3.99±4.09	1.83±0.06	3.42± 0.16	1.71±0.04
1997-05-15/01:15:21.945	RH08	449.00± 11.50	18.6±0.40	7.29±7.34	3.99±0.14	5.06± 0.11	3.14±0.07
1997-05-20/05:10:47.400	RH08	349.60± 2.60	8.60±0.30	3.39±3.52	1.92±0.13	2.02± 0.16	1.50±0.08
1997-10-24/11:18:09.966	RH08	490.90± 13.00	11.0±0.70	9.14±9.91	1.92±0.07	3.71± 0.23	1.73±0.06
1997-11-30/07:15:44.250	RH08	360.60± 4.40	19.2±0.50	4.81±5.00	3.01±0.08	3.67± 0.08	2.48±0.05
1997-12-10/04:33:14.664	RH08	391.20± 12.40	10.2±0.90	7.10±7.35	2.73±0.17	3.89± 0.26	2.26±0.10
1997-12-30/01:13:43.921	RH08	423.40± 8.10	7.70±0.20	5.37±5.82	2.47±0.07	2.94± 0.07	1.89±0.03
1998-01-06/13:29:00.368	RH08	408.40± 10.00	9.70±0.40	6.53±6.86	2.41±0.07	3.40± 0.29	1.97±0.05
1998-01-31/15:53:43.500	RH09	418.50± 20.20	6.70±0.50	9.81±9.87	1.06±0.06	3.62± 0.37	1.04±0.02
1998-03-04/11:02:45.500	MX3	455.50± 3170	4.70±0.20	3.17±3.20	3.48±0.15	3.18± 0.16	2.57±0.04
1998-04-07/16:53:35.700	RH08	368.80± 4.00	9.30±0.30	6.87±6.94	2.02±0.04	3.98± 0.15	1.92±0.03
1998-04-23/17:29:02.500	RH08	401.70± 9.80	14.3±0.80	4.18±4.22	3.22±0.10	2.32± 0.06	1.98±0.05
1998-04-30/08:43:15.291	RH08	331.20± 6.30	11.6±0.60	1.04±1.57	15.61±4.14	6.91± 0.37	6.39±0.34
1998-05-03/17:02:20.425	RH08	499.60± 11.10	3.80±0.40	3.50±3.72	1.91±0.11	5.50± 0.42	1.85±0.09
1998-05-15/13:53:46.000	RH08	328.50± 2.10	12.3±0.10	2.85±2.87	4.61±0.06	4.51± 0.15	3.40±0.04
1998-06-13/19:18:10.950	MX2	257.70± 8.00	3.70±0.40	4.45±4.50	1.86±0.13	4.70± 0.47	1.83±0.08
1998-08-06/07:16:07.587	RH08	478.80± 36.50	10.9±1.00	10.3±10.4	1.66±0.10	5.11± 0.39	1.58±0.08
1998-08-19/18:40:41.450	RH08	334.70± 6.20	7.80±0.30	3.54±3.91	2.80±0.17	3.35± 0.17	2.32±0.13
1998-08-26/06:40:24.972	RH08	687.40± 26.80	4.90±0.40	6.48±6.64	6.20±0.39	7.30± 0.28	4.74±0.18
1998-10-02/07:06:02.475	RH08	620.30± 77.00	2.80±1.10	6.48±7.15	2.88±0.91	4.02± 0.94	2.66±0.41
1998-10-23/12:58:20.505	RH09	584.60± 7.90	2.60±0.10	4.22±4.53	2.27±0.11	2.08± 0.10	1.66±0.05
1998-11-08/04:41:17.290	RH08	644.50± 64.30	4.40±0.70	17.4±17.6	1.51±0.14	6.47± 1.11	1.49±0.14
1998-12-28/18:20:16.211	RH08	465.20± 30.20	6.90±0.90	6.88±8.53	1.75±0.27	2.28± 0.55	1.42±0.16
1999-01-13/10:47:45.119	RH08	433.10± 22.40	9.70±1.10	5.06±6.24	2.48±0.27	2.69± 0.27	1.85±0.20
1999-01-22/20:21:37.150	RH08	668.90±146.50	2.90±0.10	9.56±10.1	1.44±0.04	2.31± 0.10	1.40±0.03
1999-02-18/02:48:15.800	RH08	699.00± 19.70	3.30±0.40	7.08±7.43	3.55±0.25	5.05± 1.16	3.05±0.38
1999-04-16/11:14:11.089	RH09	479.80± 14.50	4.00±0.50	6.60±6.63	1.60±0.11	3.62± 0.37	1.49±0.08
1999-05-18/00:32:39.625	RH08	442.40± 3.80	8.00±0.50	5.56±5.66	2.37±0.11	3.38± 0.19	2.25±0.07
1999-06-26/19:30:58.154	RH08	467.20± 9.70	15.6±1.00	11.9±12.9	2.22±0.07	2.93± 0.14	1.83±0.03
1999-07-02/00:27:24.060	RH08	635.90± 36.00	1.30±0.00	4.59±5.05	2.05±0.07	2.83± 0.29	1.81±0.04

Table 1 continued

Table 1 *(continued)*

Ramp Time [UTC]	RH [a] Meth.	$\langle\lvert V_{shn}\rvert\rangle_{up}$ [b] [km/s]	$\langle n_i\rangle_{up}$ [c] [cm^{-3}]	$\langle\lvert\mathbf{B}_o\rvert\rangle_{up}$ [d] [nT]	$\langle M_A\rangle_{up}$ [e]	$\langle M_{cs}\rangle_{up}$ [f]	$\langle M_f\rangle_{up}$ [g]
1999-07-06/14:24:56.625	RH08	475.70± 20.80	2.90±0.20	5.59±5.99	1.86±0.07	6.50± 0.55	1.83±0.05
1999-07-26/23:50:17.327	RH08	426.80± 8.80	2.30±0.20	3.85±4.06	1.33±0.24	1.39± 0.17	1.15±0.05
1999-08-04/01:44:38.601	RH08	418.10± 6.90	8.70±0.20	6.23±6.39	2.07±0.08	4.91± 0.27	1.95±0.04
1999-08-15/10:33:45.975	RH09	424.30± 8.90	15.5±0.60	4.49±5.49	3.73±0.26	2.35± 0.10	1.99±0.05
1999-08-23/15:41:34.980	MX2	506.20± 25.10	8.70±0.40	10.6±10.7	1.17±0.05	1.98± 0.11	1.01±0.04
1999-09-12/03:57:56.062	RH08	534.90± 8.00	3.70±0.20	4.04±4.35	3.15±0.10	3.41± 0.12	2.35±0.06
1999-09-15/07:43:49.625	RH08	665.50± 16.30	2.60±0.10	5.69±7.01	2.04±0.12	1.93± 0.07	1.42±0.06
1999-09-22/12:09:25.567	RH08	510.70± 37.20	17.0±0.70	11.3±13.8	2.44±0.10	2.85± 0.11	1.88±0.08
1999-10-21/02:20:51.968	RH08	477.30± 28.60	13.4±0.40	9.17±9.64	2.46±0.07	4.71± 0.16	2.21±0.06
1999-12-12/15:54:27.750	RH08	564.00± 39.90	0.60±0.10	4.71±4.83	1.51±0.19	7.20± 1.40	1.51±0.20
2000-02-11/23:33:55.710	RH08	641.40± 13.20	5.00±0.40	6.70±6.94	3.98±0.12	5.62± 0.25	3.25±0.08
2000-02-20/21:03:45.795	RH08	474.50± 13.40	8.60±0.50	7.64±7.70	3.06±0.10	5.48± 0.32	2.67±0.05

[a] Rankine-Hugoniot

[b] shock normal speed in SCF

[c] upstream ion number density

[d] upstream magnetic field magnitude

[e] upstream Alfvénic Mach number

[f] upstream sound Mach number

[g] upstream fast mode Mach number

NOTE—For symbol definitions, see Section 1.

3. CRITICAL MACH NUMBERS

For each crossing, we estimated four different critical Mach numbers. The first critical Mach number, M_{cr}, defines the maximum Mach number above which an ion sound wave could not phase stand within the shock ramp, thus for $\langle M_f/M_{cr}\rangle_{up} \geq 1$ the shock cannot rely upon resistive dissipation effects to maintain a stable discontinuity (e.g., Edmiston & Kennel 1984; Kennel et al. 1985). We also estimated three whistler critical Mach numbers (Krasnoselskikh et al. 2002), defined as: M_{ww} is the maximum Mach number for which a linear whistler can phase stand upstream of the shock ramp; M_{gr} is similar to M_{ww} but depends upon the whistler group velocity, thus determines the cutoff where a linear precursor can no longer carry energy into the upstream; and M_{nw} defines the separation between a stable/stationary and "breaking" shock front.

The ratios between the upstream fast mode Mach number and each critical Mach number is shown in Table 2 along with the upstream average beta and shock normal angle for the 145 good shocks. All values are reported with associated uncertainties. Notice that only 12(∼8%) satisfy $\langle M_f/M_{cr}\rangle_{up} \geq 1$, thus most of these shocks are subcritical.

As a side note, for all 250 quasi-perpendicular shocks in the WSDB, 104(∼42%) satisfy $\langle M_f/M_{cr}\rangle_{up} \geq 1$ thus slightly less than half are supercritical. Further, only 40(∼16%) satisfy $\langle M_f/M_{ww}\rangle_{up} \geq 1$, thus most quasi-perpendicular interplanetary shocks should exhibit upstream whistler precursor waves, assuming cold plasma and a dispersion-only dissipation mechanism (e.g., Krasnoselskikh et al. 2002).

Table 2. IP Shock Critical Mach Number Ratios

Ramp Time [UTC]	$\langle \lvert U_{shn} \rvert \rangle_{up}$ [a] [km/s]	$\langle \beta_{Tot} \rangle_{up}$ [b]	$\langle \theta_{Bn} \rangle_{up}$ [c] [deg]	$\langle M_f/M_{cr} \rangle_{up}$ [d]	$\langle M_f/M_{ww} \rangle_{up}$ [e]	$\langle M_f/M_{gr} \rangle_{up}$ [f]	$\langle M_f/M_{nw} \rangle_{up}$ [g]
1995-02-26/02:55:41.125	58.60± 1.00	0.19±0.19	34.80±1.50	0.67±0.05	0.08±0.00	0.06±0.00	0.05±0.00
1995-07-24/02:23:13.000	90.70± 1.10	1.21±1.27	33.80±7.00	2.62±0.85	0.23±0.02	0.17±0.02	0.16±0.01
1995-08-17/02:47:21.925	70.10± 4.40	0.89±0.94	41.90±4.10	1.03±0.31	0.11±0.01	0.08±0.01	0.08±0.01
1995-08-22/12:56:49.250	66.10± 2.50	0.65±0.67	66.10±7.40	0.91±0.24	0.21±0.06	0.16±0.05	0.15±0.04
1995-12-24/05:57:35.375	101.50± 2.30	0.29±0.26	58.40±3.30	1.14±0.16	0.22±0.03	0.17±0.02	0.16±0.02
1996-02-06/19:14:23.700	52.90± 1.30	0.42±0.43	48.40±4.60	0.70±0.13	0.10±0.01	0.08±0.01	0.07±0.01
1996-04-02/10:07:57.525	36.90± 1.00	1.39±1.47	74.00±3.10	0.71±0.27	0.22±0.04	0.17±0.03	0.15±0.03
1996-04-03/09:47:17.152	49.60± 0.80	0.39±0.38	75.70±1.40	0.71±0.12	0.30±0.03	0.23±0.02	0.21±0.02
1996-04-08/02:41:09.765	76.40± 0.70	0.23±0.23	73.30±1.10	0.87±0.10	0.34±0.02	0.26±0.02	0.24±0.02
1997-02-09/12:50:21.125	122.90± 3.50	1.37±1.30	42.70±10.2	1.19±0.40	0.12±0.02	0.09±0.02	0.08±0.01
1997-02-27/17:29:09.087	122.50± 2.50	0.17±0.18	42.20±3.50	0.80±0.06	0.11±0.01	0.08±0.00	0.08±0.00
1997-05-15/01:15:21.945	147.00± 0.80	0.38±0.38	85.30±2.20	1.38±0.24	1.79±0.84	1.38±0.64	1.27±0.59
1997-05-20/05:10:47.400	49.50± 3.20	0.54±0.54	46.00±11.3	0.80±0.18	0.10±0.02	0.08±0.02	0.07±0.02
1997-10-24/11:18:09.966	117.40± 2.40	0.16±0.16	68.30±4.50	0.71±0.06	0.22±0.04	0.17±0.03	0.15±0.03
1997-11-30/07:15:44.250	71.90± 1.20	0.41±0.40	49.10±2.10	1.24±0.21	0.18±0.01	0.14±0.01	0.13±0.01
1997-12-10/04:33:14.664	132.30± 2.30	0.30±0.28	70.90±1.60	0.99±0.14	0.32±0.03	0.25±0.02	0.23±0.02
1997-12-30/01:13:43.921	107.20± 1.30	0.42±0.41	87.40±8.10	0.85±0.16	0.81±0.53	0.62±0.41	0.57±0.37
1998-01-06/13:29:00.368	111.00± 2.60	0.30±0.30	82.30±6.20	0.84±0.12	0.69±0.55	0.53±0.43	0.49±0.39
1998-01-31/15:53:43.500	87.30± 3.50	0.05±0.05	37.50±2.50	0.48±0.02	0.06±0.00	0.05±0.00	0.04±0.00
1998-03-04/11:02:45.500	110.40± 0.30	0.73±0.76	41.70±3.00	1.48±0.39	0.16±0.01	0.12±0.01	0.11±0.01
1998-04-07/16:53:35.700	99.70± 0.70	0.16±0.16	37.10±0.90	0.93±0.06	0.11±0.00	0.09±0.00	0.08±0.00
1998-04-23/17:29:02.500	77.70± 1.20	1.15±1.17	51.70±1.60	1.16±0.39	0.15±0.01	0.11±0.00	0.11±0.00
1998-04-30/08:43:15.291	114.40± 1.80	3.86±2.65	64.60±9.30	5.14±0.89	0.70±0.24	0.54±0.19	0.50±0.17
1998-05-03/17:02:20.425	76.80± 2.90	0.07±0.08	52.30±2.00	0.78±0.05	0.14±0.01	0.11±0.01	0.10±0.01
1998-05-15/13:53:46.000	83.30± 0.60	0.63±0.62	52.70±1.80	1.79±0.43	0.26±0.01	0.20±0.01	0.19±0.01
1998-06-13/19:18:10.950	95.20± 2.20	0.10±0.08	27.20±2.50	0.93±0.05	0.10±0.00	0.07±0.00	0.07±0.00
1998-08-06/07:16:07.587	113.90± 1.90	0.06±0.07	80.80±3.90	0.60±0.04	0.46±0.20	0.36±0.15	0.33±0.14
1998-08-19/18:40:41.450	78.10± 2.80	0.42±0.41	45.50±8.10	1.19±0.22	0.16±0.02	0.12±0.02	0.11±0.02
1998-08-26/06:40:24.972	401.30± 3.80	0.44±0.42	82.20±3.00	2.15±0.41	1.63±0.63	1.26±0.48	1.15±0.44
1998-10-02/07:06:02.475	270.70± 10.10	0.44±0.37	26.20±9.90	1.58±0.35	0.14±0.02	0.11±0.02	0.10±0.02
1998-10-23/12:58:20.505	131.30± 5.40	0.72±0.74	43.60±8.40	0.94±0.25	0.11±0.02	0.08±0.01	0.08±0.01
1998-11-08/04:41:17.290	275.10± 6.10	0.03±0.03	54.60±1.40	0.61±0.06	0.12±0.01	0.09±0.01	0.08±0.01
1998-12-28/18:20:16.211	105.90± 10.90	0.41±0.43	60.70±12.9	0.68±0.15	0.14±0.06	0.11±0.04	0.10±0.04
1999-01-13/10:47:45.119	92.90± 7.30	0.52±0.49	70.90±12.7	0.89±0.21	0.27±0.18	0.21±0.14	0.19±0.12
1999-01-22/20:21:37.150	180.20± 3.50	0.23±0.23	17.10±5.70	0.83±0.08	0.07±0.00	0.05±0.00	0.05±0.00
1999-02-18/02:48:15.800	304.40± 20.30	0.31±0.23	51.30±6.80	1.45±0.24	0.23±0.04	0.18±0.03	0.16±0.03
1999-04-16/11:14:11.089	116.30± 4.20	0.12±0.11	62.30±3.40	0.61±0.05	0.15±0.02	0.12±0.01	0.11±0.01
1999-05-18/00:32:39.625	102.20± 0.60	0.30±0.28	22.20±1.00	1.31±0.15	0.11±0.00	0.09±0.00	0.08±0.00
1999-06-26/19:30:58.154	145.40± 1.70	0.34±0.36	59.40±3.70	0.85±0.13	0.17±0.02	0.13±0.01	0.12±0.01
1999-07-02/00:27:24.060	178.80± 5.30	0.32±0.31	39.30±6.60	0.93±0.13	0.11±0.01	0.08±0.01	0.08±0.01
1999-07-06/14:24:56.625	135.80± 3.10	0.05±0.05	44.80±6.60	0.80±0.04	0.12±0.01	0.09±0.01	0.09±0.01
1999-07-26/23:50:17.327	75.80± 7.60	0.60±0.79	18.50±9.10	0.77±0.18	0.06±0.00	0.04±0.00	0.04±0.00

Table 2 continued

Table 2 *(continued)*

Ramp Time [UTC]	$\langle \lvert U_{shn} \rvert \rangle_{up}$ [a] [km/s]	$\langle \beta_{Tot} \rangle_{up}$ [b]	$\langle \theta_{Bn} \rangle_{up}$ [c] [deg]	$\langle M_f / M_{cr} \rangle_{up}$ [d]	$\langle M_f / M_{ww} \rangle_{up}$ [e]	$\langle M_f / M_{gr} \rangle_{up}$ [f]	$\langle M_f / M_{nw} \rangle_{up}$ [g]
1999-08-04/01:44:38.601	95.90± 2.90	0.11±0.11	54.10±4.80	0.83±0.05	0.16±0.02	0.12±0.01	0.11±0.01
1999-08-15/10:33:45.975	95.10± 1.30	1.55±1.60	79.20±4.30	1.11±0.44	0.50±0.20	0.38±0.15	0.35±0.14
1999-08-23/15:41:34.980	92.30± 3.50	0.21±0.21	88.60±4.40	0.41±0.05	0.80±0.52	0.61±0.40	0.56±0.37
1999-09-12/03:57:56.062	145.30± 3.50	0.51±0.50	69.90±5.40	1.12±0.24	0.32±0.08	0.25±0.06	0.23±0.06
1999-09-15/07:43:49.625	163.70± 2.70	0.68±0.73	73.60±4.30	0.70±0.19	0.24±0.06	0.18±0.05	0.17±0.04
1999-09-22/12:09:25.567	149.20± 3.40	0.44±0.46	70.80±3.40	0.87±0.18	0.27±0.05	0.21±0.04	0.19±0.03
1999-10-21/02:20:51.968	135.80± 1.10	0.17±0.16	69.40±3.30	0.91±0.08	0.29±0.05	0.23±0.04	0.21±0.03
1999-12-12/15:54:27.750	203.90± 8.50	0.03±0.03	48.70±3.00	0.63±0.09	0.11±0.02	0.08±0.01	0.08±0.01
2000-02-11/23:33:55.710	263.60± 2.40	0.30±0.30	86.50±2.20	1.38±0.20	2.49±1.56	1.91±1.20	1.76±1.10
2000-02-20/21:03:45.795	174.60± 2.70	0.19±0.18	88.10±4.60	1.08±0.10	1.93±1.28	1.49±0.99	1.37±0.91

[a] shock normal speed in SHF

[b] upstream plasma beta

[c] shock normal angle

[d] fast mode to first critical Mach number ratio

[e] fast mode to linear (phase) whistler critical Mach number

[f] fast mode to linear (group) whistler critical Mach number

[g] fast mode to nonlinear whistler critical Mach number

Note—For symbol definitions, see Section 1.

4. DATA AVAILABILITY

Most relevant *Wind* instrument data can be found on CDAWeb at:
http://cdaweb.gsfc.nasa.gov
including quasi-static magnetic fields from *Wind*/MFI (Lepping et al. 1995) and solar wind plasma parameters from the *Wind*/SWE Faraday Cups (FCs) (Ogilvie et al. 1995). The remaining *Wind*/3DP level-zero (lz) data can be found at:
http://sprg.ssl.berkeley.edu/wind3dp/data/wi/3dp/lz/.

The Harvard Smithsonian Center for Astrophysics' *Wind* interplanetary shock list can be found at:
https://www.cfa.harvard.edu/shocks/wi_data/.

The critical Mach number analysis software can be found at:
https://github.com/pulupa/Critical-Mach.

Any additional analysis software can be found at:
https://github.com/lynnbwilsoniii/wind_3dp_pros.

5. EXTRA STATISTICAL RESULTS

In the following one-variable statistics and distributions of $T_{s,j}$, n_s, $\beta_{es,j}$, and $(T_s/T_{s'})_j$ are presented that are not directly shown in the main multi-part papers. Given that none of the parameters have Gaussian distributions, the median ($\tilde{X}$) and lower ($X_{25\%}$) and upper quartile ($\equiv X_{75\%}$) values in addition to the minimum (X_{min}), maximum (X_{max}), and mean ($\bar{X}$) in the statistical tables shown in the main paper. The distributions for these parameters are shown in the histograms in Figures 1–8.

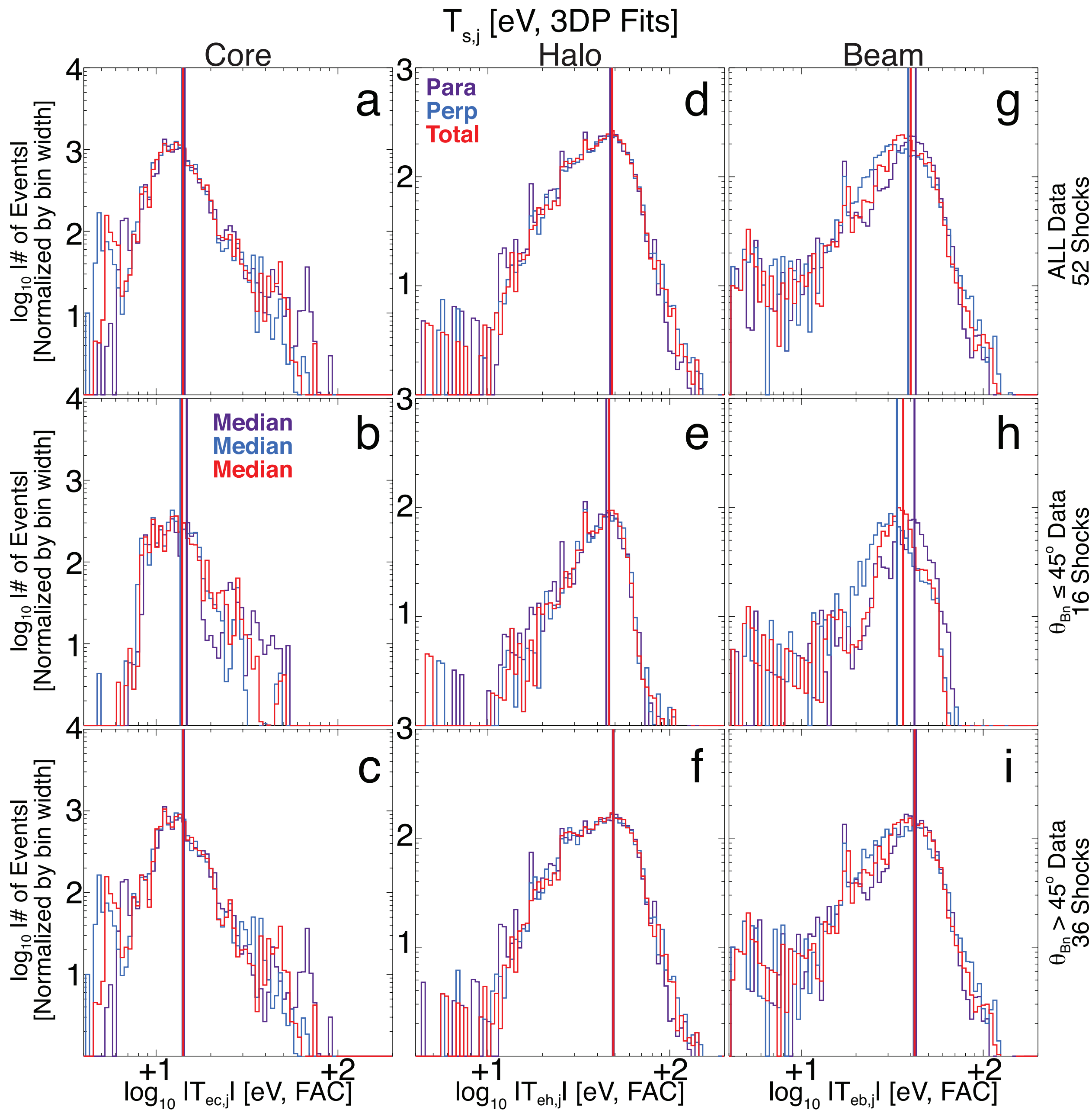

Figure 1. Temperatures [eV] for different electron components in each column and for the different shock geometries (i.e., rows) shown to the right. In each panel, there are three color-coded histograms for the different field-aligned components defined as follows: total (red); parallel (violet); and perpendicular (blue). The color-coded vertical lines are the median values of the regridded distributions for the corresponding color-coded histograms.

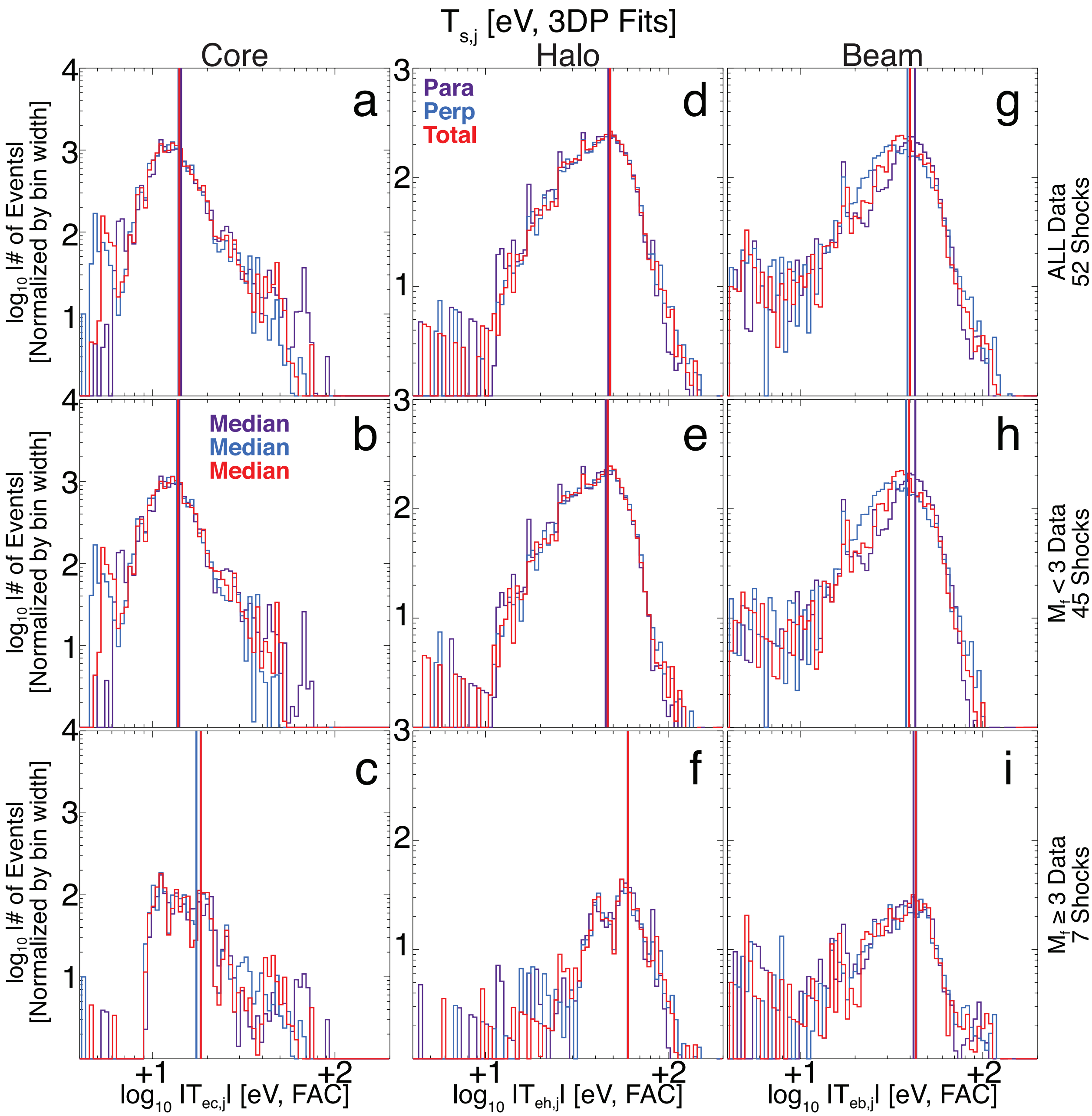

Figure 2. Temperatures [eV] for different electron components in each column and for the different Mach numbers (i.e., rows) shown to the right with the same format as Figure 1.

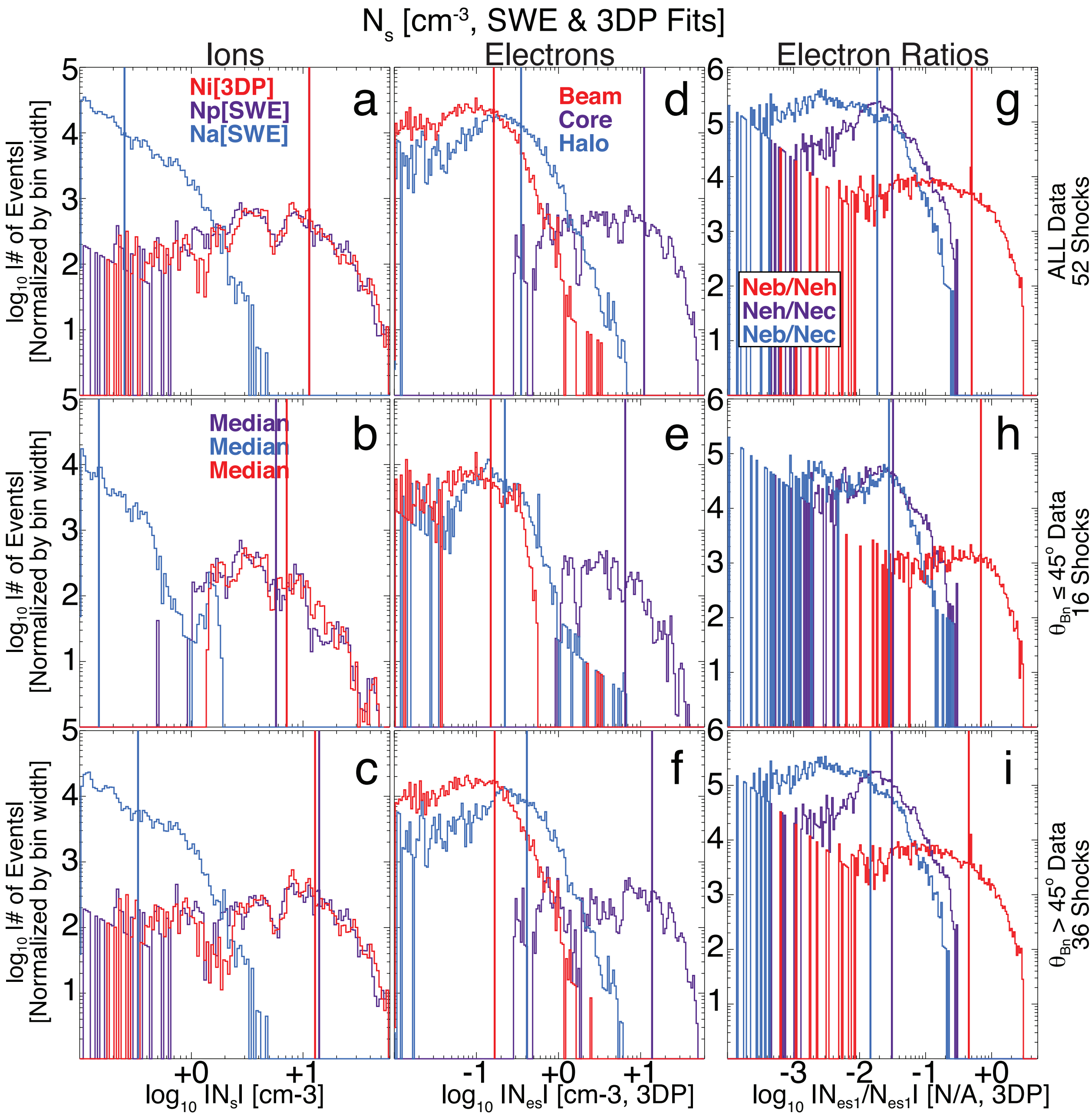

Figure 3. Densities $[cm^{-3}]$ and density ratios for different ion and electron components. The format is similar to Figure 1 with the row organization but the columns differ. The first column here shows proton (violet) and alpha-particle (blue) density from *Wind*/SWE and total ion density from *Wind*/3DP (red). The second column shows n_{es} for the core (violet), halo (blue), and beam/strahl (red) components. The third column shows n_{es1}/n_{es2} for the halo-to-core (violet), beam-to-core (blue), and beam-to-halo (red) density ratios.

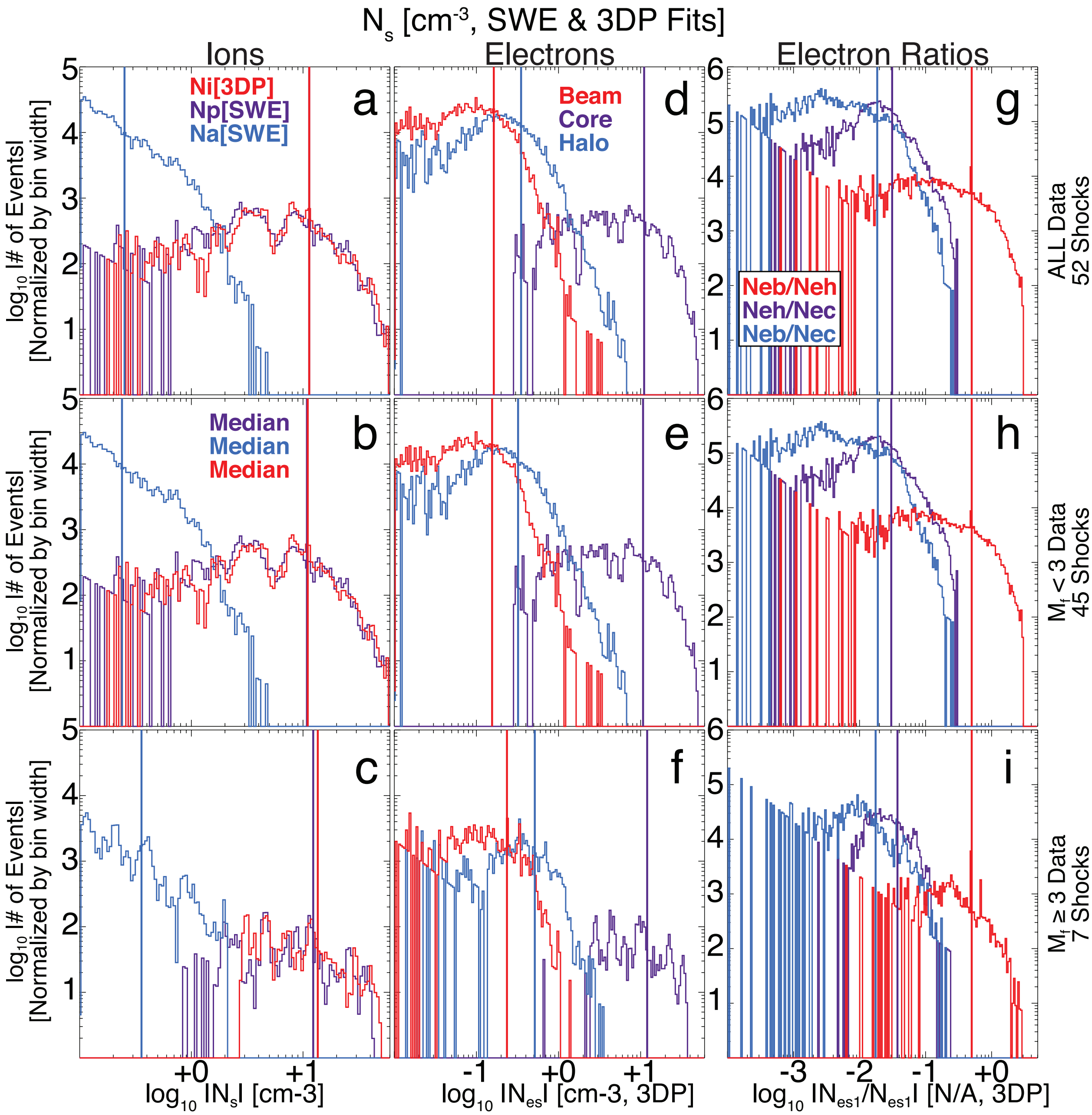

Figure 4. The same format and variables as in Figure 3 but for different Mach numbers instead of geometry.

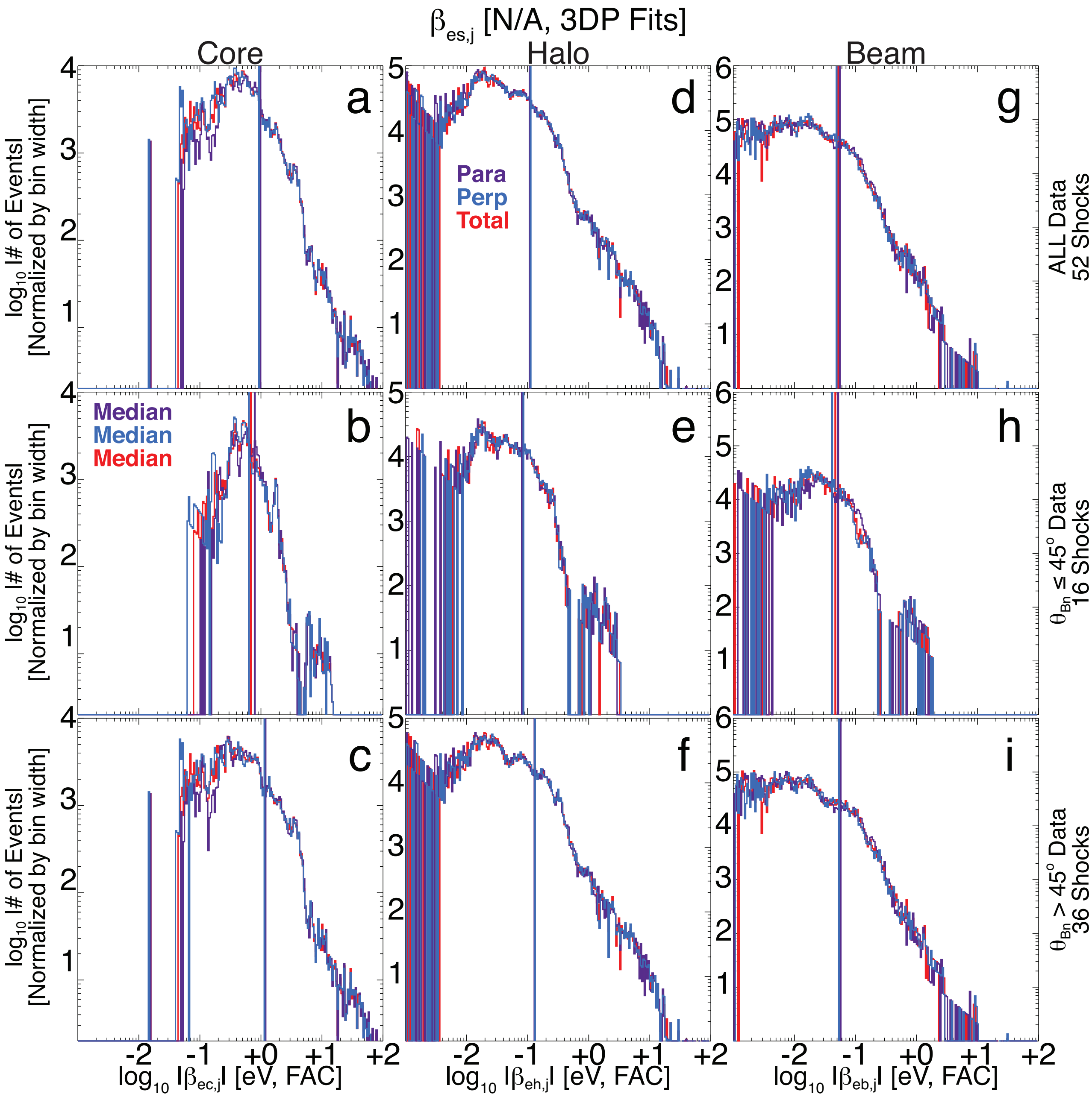

Figure 5. The same format as Figures 1 and 3 except for electron betas [N/A]. Note that all three components have different vertical axis scales.

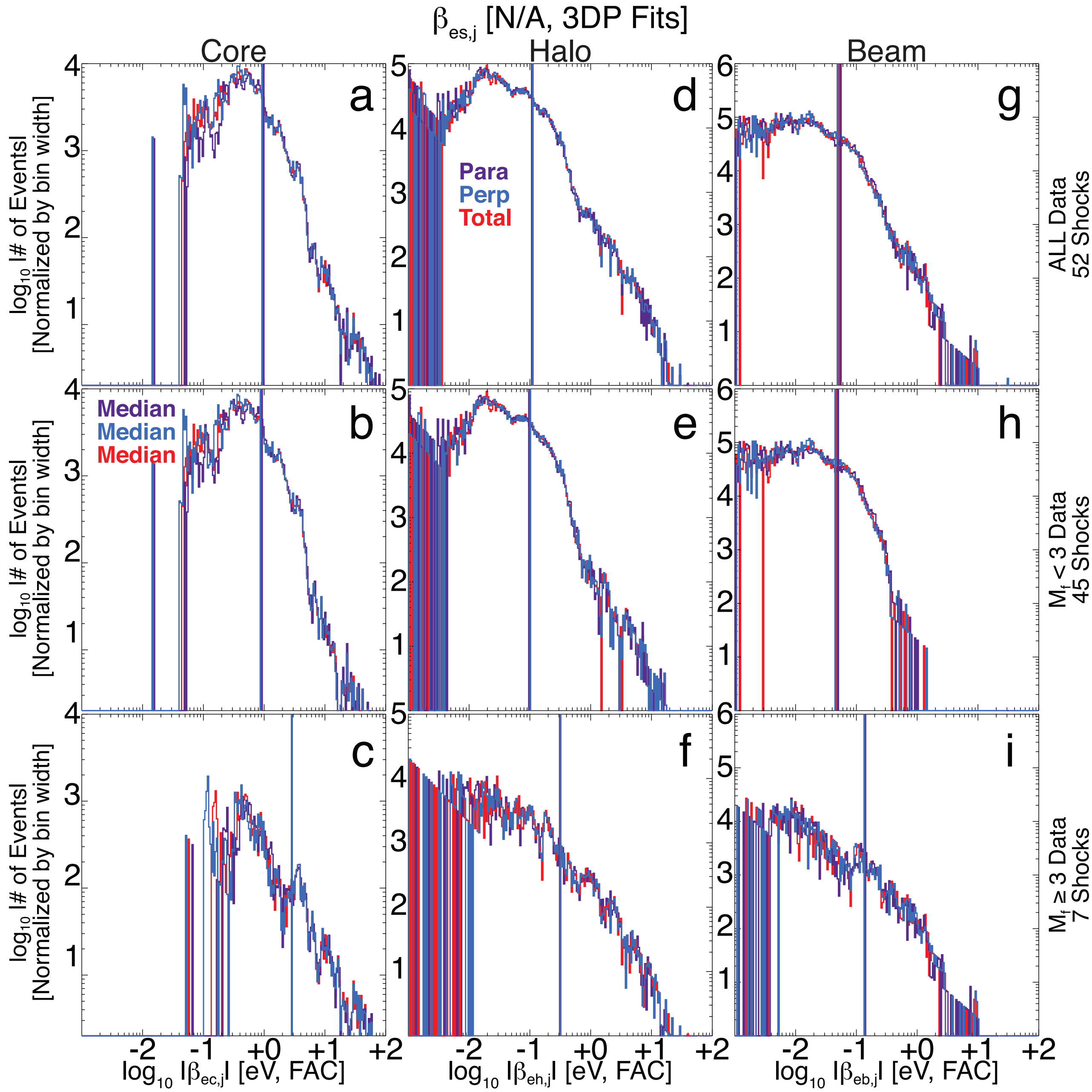

Figure 6. The same format as Figure 5 except for different Mach numbers (i.e., rows) instead of geometry. Note that all three components have different vertical axis scales.

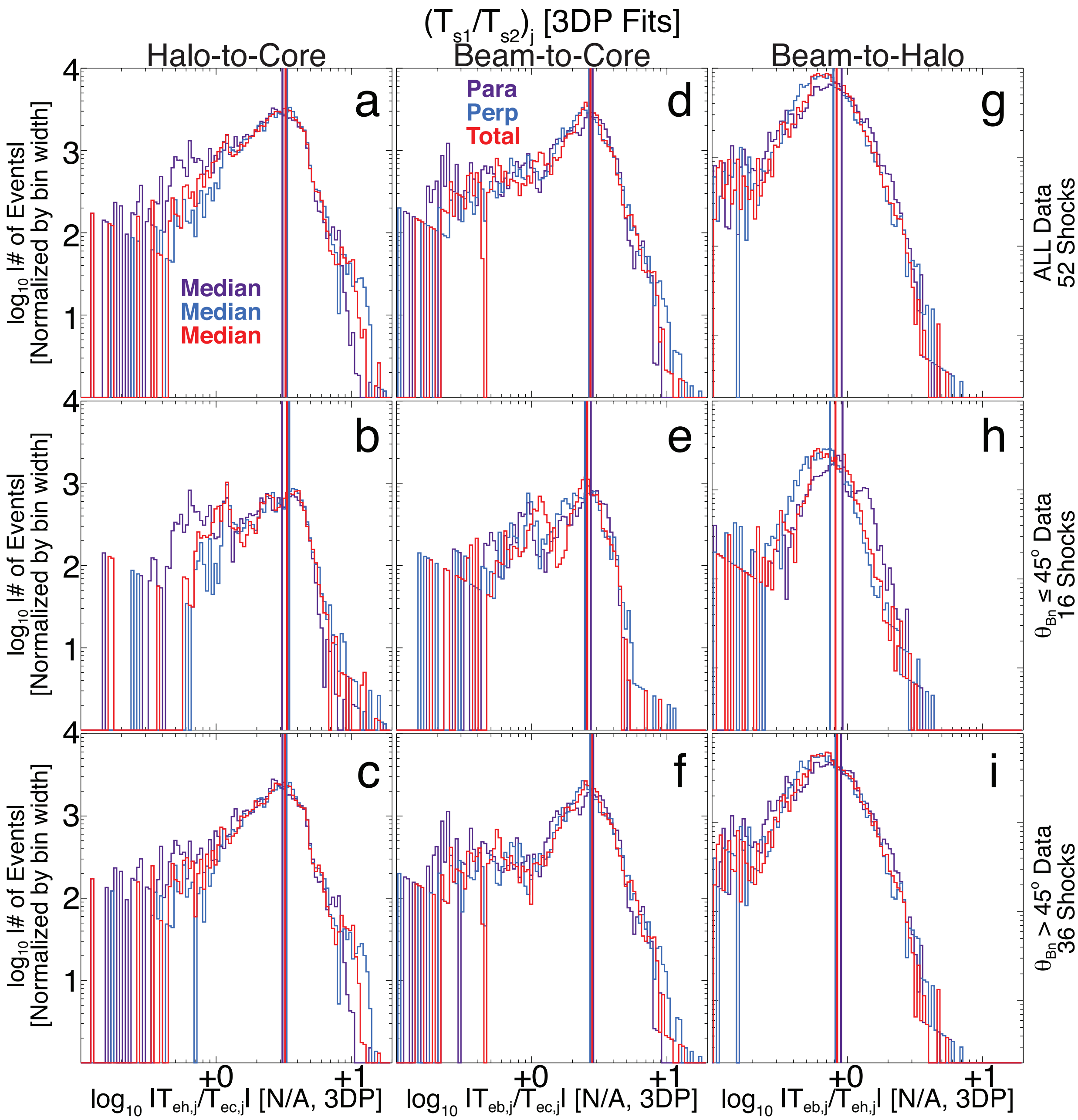

Figure 7. The same format as Figure 1 except for electron temperature ratios [N/A]. Note that all three components have a uniform vertical axis scale.

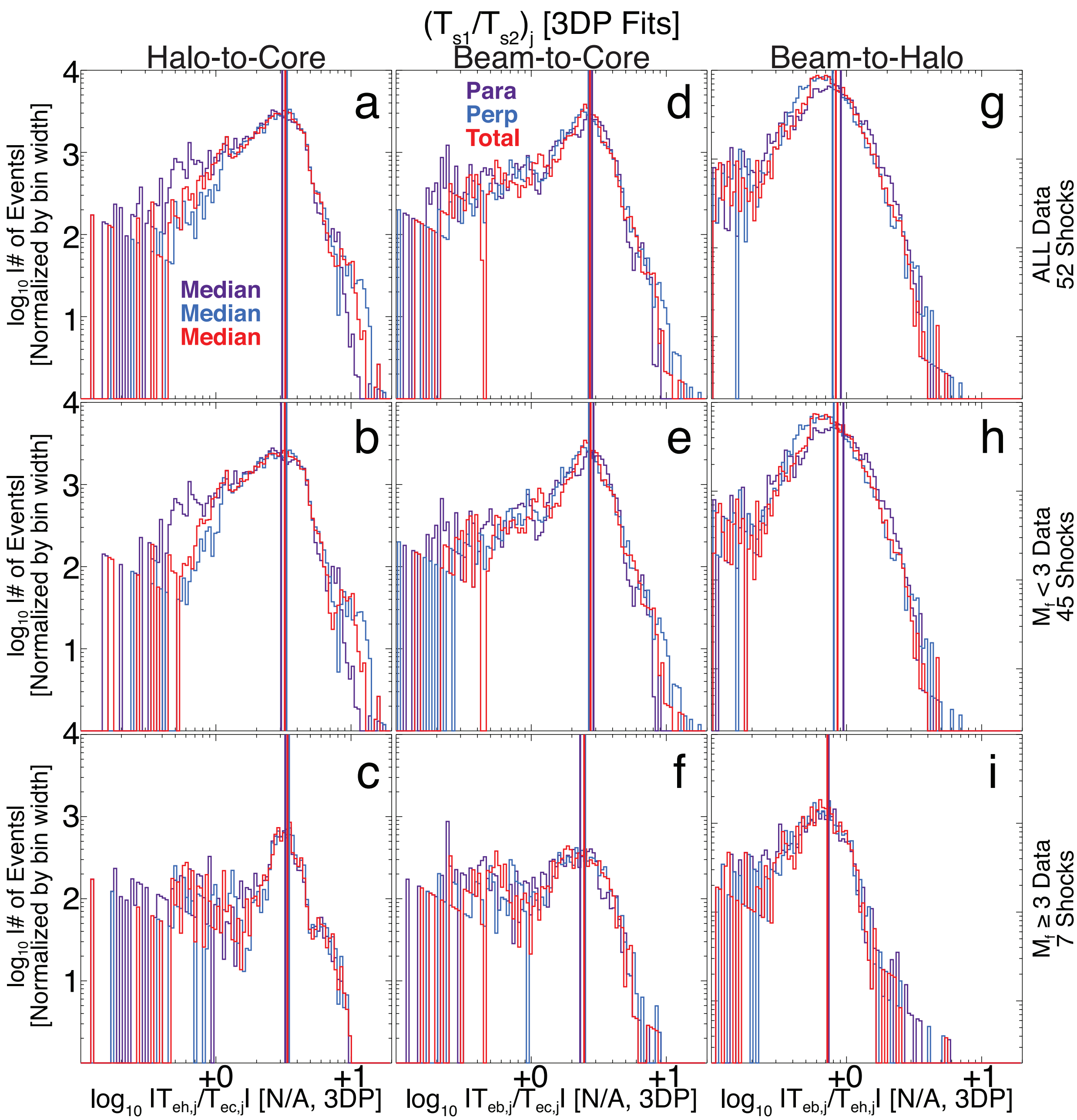

Figure 8. The same format as Figure 2 except for electron temperature ratios [N/A]. Note that all three components have a uniform vertical axis scale.

APPENDIX

A. VELOCITY DISTRIBUTION FUNCTIONS

A generalized Gaussian probability density function is defined as:

$$f_s(x) = \frac{A_o}{\sqrt{2\pi\sigma^2}}\, e^{-\frac{(x-x_o)^2}{2\sigma^2}} \tag{A1}$$

where x_o is the displacement of the peak from x = 0, A_o is a normalization amplitude, s denotes the specific set (later used for particle species) of data the distribution describes, and σ^2 is the variance. For this distribution, the Full Width at Half Maximum (FWHM) is given by:

$$FWHM = 2\sqrt{2\ln 2}\,\sigma \tag{A2}$$

Introducing the change of variable x → v, where v is a velocity, then the distribution in Equation A1 becomes a Maxwell-Boltzmann velocity distribution, or Maxwellian, given by:

$$f_s(v) = \frac{n_o}{\sqrt{\pi}\,V_{Ts}}\, e^{-\left(\frac{v-v_o}{V_{Ts}}\right)^2} \tag{A3}$$

where v_o is the drift speed of the peak relative to zero, n_o is the particle number density, and $2\sigma^2 \to {V_{Ts}}^2$, i.e., the thermal speed given by a one-dimensional most probable speed of a Gaussian distribution, which is related to the FWHM by $2\sqrt{\ln 2}\,V_{Ts}$.

The general representation of a two dimensional multivariate distribution is given by the following:

$$f(x,y) = \alpha\, e^{-\left(\frac{\beta}{\sqrt{2(1-\rho^2)}}\right)^2} \tag{A4a}$$

where α and β are given by

$$\alpha = \frac{A_o}{2\pi\sigma_x\sigma_y\sqrt{1-\rho^2}} \tag{A4b}$$

$$\beta^2 = \left[\left(\frac{x-x_o}{\sigma_x}\right)^2 + \left(\frac{y-y_o}{\sigma_y}\right)^2 - \left(\frac{2\rho(x-x_o)(y-y_o)}{\sigma_x\sigma_y}\right)\right] \tag{A4c}$$

and ρ and σ_j are defined in the following manner:

$$\rho = \frac{cov(x,y)}{\sigma_x\sigma_y} \tag{A4d}$$

$$cov(x,y) = E\left[(x-\mu_x)(y-\mu_y)\right] \tag{A4e}$$

Here ρ is the correlation between x and y, $\mu_x = E[X]$ is the expected value of the aggregate data set $X = \cup_i\, x_i$. In the limit $\rho \to 0$ (i.e., x and y are uncorrelated), Equation A4a reduces to:

$$f(x,y) = \frac{A_x A_y}{2\pi\sigma_x\sigma_y}\, e^{-\frac{1}{2}\left[\left(\frac{x-\mu_x}{\sigma_x}\right)^2 + \left(\frac{y-\mu_y}{\sigma_y}\right)^2\right]} \tag{A5}$$

A.1. *Bi-Maxwellian Distributions*

In general, for uncorrelated variables, one can write:

$$f(x, y, z) = f(x)\, f(y)\, f(z) \tag{A6}$$

and assuming gyrotropy one finds $V_x \rightarrow V_\perp \cos\phi$, $V_y \rightarrow V_\perp \sin\phi$, and $V_z \rightarrow V_\parallel$, where ϕ is the phase angle of the velocity and $\partial f / \partial \phi = 0$. One can show that such a gyrotropic distribution satisfies $V_{T\perp,x} = V_{T\perp,y} \equiv V_{T\perp}$. Substituting the following into Equation A5, x $\rightarrow V_\parallel$, y $\rightarrow V_\perp$, $\mu_j \rightarrow V_{o,j}$, and $\sigma_j \rightarrow V_{T,j}/\sqrt{2}$, yields a bi-Maxwellian velocity distribution function (VDF) given by:

$$f(V_\parallel, V_\perp) = \frac{n_o}{\pi^{3/2} {V_{T\perp}}^2 V_{T\parallel}}\, e^{-\left[\left(\frac{V_\parallel - v_{o\parallel}}{V_{T\parallel}}\right)^2 + \left(\frac{V_\perp - v_{o\perp}}{V_{T\perp}}\right)^2\right]} \tag{A7}$$

The bi-Maxwellian is the most commonly used VDF to model both ions and electrons in space plasmas (e.g., Feldman et al. 1979b,a, 1983a; Kasper et al. 2006).

A.1.1. *Derivatives of Parameters: Bi-Maxwellian Distributions*

In the use of numerical methods like the Levenberg-Marquardt algorithm (e.g., Markwardt 2009), it is useful to define the derivatives of a function with respect to the free parameters. In the case of velocity distributions, these are the density, thermal speeds, drift speeds, and exponent (for self-similar and kappa distributions discussed below). First, some simplifying terms are defined for brevity, given by:

$$u_j = V_j - v_{oj} \tag{A8a}$$

$$w_j = \frac{u_j}{V_{Tj}} \tag{A8b}$$

$$\psi(z) = \frac{\Gamma'(z)}{\Gamma(z)} \equiv \text{digamma function} \tag{A8c}$$

where $\Gamma(z)$ is the Riemann gamma function of argument z. After denoting the VDF in Equation A7 as $f^{(m)}$, the partial derivatives are given by:

$$\frac{\partial f^{(m)}}{\partial n_o} = \frac{f^{(m)}}{n_o} \tag{A9a}$$

$$\frac{\partial f^{(m)}}{\partial V_{T\parallel}} = \left[\frac{2\ \left({w_\parallel}^2 - 1\right)}{V_{T\parallel}}\right] f^{(m)} \tag{A9b}$$

$$\frac{\partial f^{(m)}}{\partial V_{T\perp}} = \left[\frac{2\ \left({w_\perp}^2 - 1\right)}{V_{T\perp}}\right] f^{(m)} \tag{A9c}$$

$$\frac{\partial f^{(m)}}{\partial v_{o\parallel}} = \left(\frac{2\ w_\parallel}{V_{T\parallel}}\right) f^{(m)} \tag{A9d}$$

$$\frac{\partial f^{(m)}}{\partial v_{o\perp}} = \left(\frac{2\ w_\perp}{V_{T\perp}}\right) f^{(m)} \tag{A9e}$$

A.2. *Bi-Kappa Distributions*

A generalized power-law particle distribution is given by a bi-kappa VDF (e.g., Livadiotis 2015; Mace & Sydora 2010), for electrons here as:

$$f(V_\perp, V_\parallel) = A_\kappa \left\{1 + \frac{1}{\left(\kappa - \frac{3}{2}\right)}\left[\left(\frac{V_\parallel - v_{o\parallel}}{V_{T\parallel}}\right)^2 + \left(\frac{V_\perp - v_{o\perp}}{V_{T\perp}}\right)^2\right]\right\}^{-(\kappa+1)} \tag{A10a}$$

where A_κ is given by

$$A_\kappa = \left[\frac{1}{\pi \left(\kappa - \frac{3}{2} \right)} \right]^{3/2} \frac{n_o \, \Gamma \left(\kappa + 1 \right)}{V_{T\perp}{}^2 \, V_{T\parallel} \, \Gamma \left(\kappa - \frac{1}{2} \right)} \tag{A10b}$$

(A10c)

where $\Gamma(z)$ is the Riemann gamma function of argument z and V_{Tj} is again the most probable speed of a 1D Gaussian for consistency, i.e., it does not depend upon κ.

The kappa velocity distribution has gained popularity in recent years owing to improvements in particle detectors and the ubiquitous non-Maxwellian tails observed for both ions and electrons (e.g., Lazar et al. 2015b,a, 2016, 2017, 2018; Livadiotis 2015; Livadiotis et al. 2018; Mace & Sydora 2010; Pulupa et al. 2014; Saeed et al. 2017; Shaaban et al. 2018), but references to and use of kappa or kappa-like (e.g., modified Lorentzian) distributions have been around for decades (e.g., Feldman et al. 1983b; Maksimovic et al. 1997; Salem et al. 2003; Vasyliunas 1968). It is beyond the scope of this study to explain the physical interpretation/origin of this function but there are several detailed discussions already published on the topic (e.g., Livadiotis 2015; Livadiotis et al. 2018).

A.2.1. *Derivatives of Parameters: Bi-Kappa Distributions*

Similar to Appendix A.1.1, the analytical derivatives for the bi-kappa VDF are shown below. Again, the following simplifying terms are defined for brevity as:

$$u_j = V_j - v_{oj} \tag{A11a}$$

$$w_j = \frac{u_j}{V_{Tj}} \tag{A11b}$$

$$\psi\left(z\right) = \frac{\Gamma'\left(z\right)}{\Gamma\left(z\right)} \equiv \text{digamma function} \tag{A11c}$$

$$D\left(w_\parallel, w_\perp, \kappa\right) = w_\parallel{}^2 + w_\perp{}^2 + \left(\kappa - \tfrac{3}{2}\right) \tag{A11d}$$

where $\Gamma(z)$ is the Riemann gamma function of argument z. After denoting the VDF in Equation A10a as $f^{(\kappa)}$, the partial derivatives are given by:

$$\frac{\partial f^{(\kappa)}}{\partial n_o} = \frac{f^{(\kappa)}}{n_o} \tag{A12a}$$

$$\frac{\partial f^{(\kappa)}}{\partial V_{T\parallel}} = \left[\frac{2 \, w_\parallel{}^2 \, \left(\kappa + \frac{1}{2}\right) - w_\perp{}^2 - \left(\kappa - \frac{3}{2}\right)}{V_{T\parallel} \, D\left(w_\parallel, w_\perp, \kappa\right)} \right] f^{(\kappa)} \tag{A12b}$$

$$\frac{\partial f^{(\kappa)}}{\partial V_{T\perp}} = \left\{ \frac{2 \, \left[\kappa \, w_\perp{}^2 - w_\parallel{}^2 - \left(\kappa - \frac{3}{2}\right)\right]}{V_{T\perp} \, D\left(w_\parallel, w_\perp, \kappa\right)} \right\} f^{(\kappa)} \tag{A12c}$$

$$\frac{\partial f^{(\kappa)}}{\partial V_{o\parallel}} = \left[\frac{2 \, w_\parallel \, \left(\kappa + 1\right)}{V_{T\parallel} \, D\left(w_\parallel, w_\perp, \kappa\right)} \right] f^{(\kappa)} \tag{A12d}$$

$$\frac{\partial f^{(\kappa)}}{\partial V_{o\perp}} = \left[\frac{2 \, w_\perp \, \left(\kappa + 1\right)}{V_{T\perp} \, D\left(w_\parallel, w_\perp, \kappa\right)} \right] f^{(\kappa)} \tag{A12e}$$

$$\frac{\partial f^{(\kappa)}}{\partial \kappa} = \left\{ \frac{\left(w_\parallel{}^2 + w_\perp{}^2\right)\left(\kappa - \frac{1}{2}\right) - \frac{3}{2} \, \left(\kappa - \frac{3}{2}\right)}{\left(\kappa - \frac{3}{2}\right) \, D\left(w_\parallel, w_\perp, \kappa\right)} - \ln\left|1 + \frac{w_\parallel{}^2 + w_\perp{}^2}{\left(\kappa - \frac{3}{2}\right)}\right| + \psi\left(\kappa + 1\right) - \psi\left(\kappa - \tfrac{1}{2}\right) \right\} f^{(\kappa)} \tag{A12f}$$

A.3. *Self-Similar Distributions*

When a VDF evolves under the action of inelastic scattering (e.g., Dum et al. 1974; Dum 1975; Goldman 1984; Horton et al. 1976; Horton & Choi 1979; Jain & Sharma 1979) or flows through disordered porous media (e.g., Matyka et al. 2016), the result is called a *self-similar distribution*, which in one dimension is given by:

$$f_s\left(x, t\right) = C_o \ e^{-\left(\frac{x}{x_o}\right)^s} \tag{A13}$$

The constant C_o is determined by by defining:

$$\begin{aligned} n_o &= \int_{-\infty}^{\infty} dv \ f_s\left(v, t\right) &\text{(A14a)} \\ &= 2 \int_{0}^{\infty} dv \ f_s\left(v, t\right) \ \text{(if symmetric)} &\text{(A14b)} \end{aligned}$$

The general solution to Equation A14b is given by:

$$\int_{0}^{\infty} dx \ x^n \ e^{-\alpha \ x^s} = \frac{\Gamma\left(k\right)}{s \ \alpha^k} \tag{A15}$$

for $n >$ -1, $s > 0$, $\alpha > 0$, and $k = (n+1)/s$. For $n = 0$, the constant C_o reduces to:

$$C_o = \frac{n_o \ s \ \alpha^{1/s}}{2 \ \Gamma\left(1/s\right)} \tag{A16}$$

Physically one can see that $\alpha \rightarrow {V_{T_s}}^{-s}$, which leads to the one dimensional form of the self-similar VDF can be given by:

$$f_s\left(v, t\right) = \frac{n_o \ s}{2 \ V_{T_s} \ \Gamma\left(1/s\right)} \ e^{-\left(\frac{v}{V_{T_s}}\right)^s} \tag{A17}$$

Note that in the limit as $s \rightarrow 2$, Equation A17 reduces to a one-dimensional Maxwellian given by Equation A3. For the 3D case, the self-similar VDF, for even integer s, reduces to:

$$f\left(V_x, V_y, V_z\right) = \left[\frac{s}{2\Gamma\left(\frac{n+1}{s}\right)}\right]^3 \frac{n_o}{\left(V_{T_x} \ V_{T_y} \ V_{T_z}\right)^{n+1}} \ e^{-\left[\left(\frac{V_x}{V_{T_x}}\right)^s + \left(\frac{V_y}{V_{T_y}}\right)^s + \left(\frac{V_z}{V_{T_z}}\right)^s\right]} \tag{A18}$$

Following the same procedure that led to Equation A7, one finds (for $n \rightarrow 0$, i.e., the zeroth moment):

$$f\left(V_\parallel, V_\perp\right) = \left[\frac{s}{2\Gamma\left(\frac{1}{s}\right)}\right]^3 \frac{n_o}{{V_{T\perp}}^2 V_{T\parallel}} \ e^{-\left[\left(\frac{V_\parallel}{V_{T\parallel}}\right)^s + \left(\frac{V_\perp}{V_{T\perp}}\right)^s\right]} \tag{A19}$$

After recalling that $\Gamma\left(1/s\right)/s = \Gamma\left(1+1/s\right)$ and letting $V_j \rightarrow V_j$ - v_{oj}, Equation A19 reduces to:

$$f\left(V_\parallel, V_\perp\right) = \left[2\Gamma\left(\frac{1+s}{s}\right)\right]^{-3} \frac{n_o}{{V_{T\perp}}^2 V_{T\parallel}} \ e^{-\left[\left(\frac{V_\parallel - v_{o\parallel}}{V_{T\parallel}}\right)^s + \left(\frac{V_\perp - v_{o\perp}}{V_{T\perp}}\right)^s\right]} \tag{A20}$$

Note that V_{Tj} is again the most probable speed of a 1D Gaussian for consistency, i.e., it does not depend upon s. Further, one can see that Equation A20 reduces to Equation A7 in the limit where $s \rightarrow 2$. A slightly more general approach can be taken where the exponents are not uniform, e.g., one assumes:

$$f\left(V_{x}, V_{y}, V_{z}\right) = C_{o} \ e^{-\left[\left(\frac{V_{x}}{V_{T_x}}\right)^{p} + \left(\frac{V_{y}}{V_{T_y}}\right)^{q} + \left(\frac{V_{z}}{V_{T_z}}\right)^{r}\right]} \tag{A21}$$

The triple integral of Equation A21, still assuming we set the result equal to n_o and assuming the integrals are symmetric about zero, results in the following:

$$n_o = 2^3 \ C_o \ V_{T_x} \ V_{T_y} \ V_{T_z} \ \Gamma\left(1 + p^{-1}\right) \ \Gamma\left(1 + q^{-1}\right) \ \Gamma\left(1 + r^{-1}\right) \tag{A22}$$

Equation A22 can be further reduced by assuming gyrotropy about the mean magnetic field direction such that $r \rightarrow q$, $V_{T_z} \rightarrow V_{T_y}$, $V_{z} \rightarrow V_{y}$, and $x \rightarrow \parallel$ and $y \rightarrow \perp$, then the expression for the normalization constant is given by:

$$C_o = \frac{p \ q^2 \ n_o}{2^3 \ V_{T_\parallel} \ {V_{T_\perp}}^{2} \ \Gamma\left(p^{-1}\right) \ \Gamma^2\left(q^{-1}\right)} \tag{A23}$$

Thus, the full bi-self-similar VDF for non-homogenous exponents is given by:

$$f\left(V_{\parallel}, V_{\perp}\right) = \frac{p \ q^2 \ n_o}{2^3 \ V_{T_\parallel} \ {V_{T_\perp}}^{2} \ \Gamma\left(p^{-1}\right) \ \Gamma^2\left(q^{-1}\right)} \ e^{-\left[\left(\frac{V_{\parallel} - v_{o\parallel}}{V_{T\parallel}}\right)^{p} + \left(\frac{V_{\perp} - v_{o\perp}}{V_{T\perp}}\right)^{q}\right]} \tag{A24a}$$

or in another form as:

$$f\left(V_{\parallel}, V_{\perp}\right) = \frac{n_o \ \Gamma^{-1}\left(\frac{1+p}{p}\right) \ \Gamma^{-2}\left(\frac{1+q}{q}\right)}{2^3 \ V_{T_\parallel} \ {V_{T_\perp}}^{2}} \ e^{-\left[\left(\frac{V_{\parallel} - v_{o\parallel}}{V_{T\parallel}}\right)^{p} + \left(\frac{V_{\perp} - v_{o\perp}}{V_{T\perp}}\right)^{q}\right]} \tag{A24b}$$

A.3.1. *Derivatives of Parameters: Self-Similar Distributions*

Similar to Appendix A.1.1, the analytical derivatives for the bi-self-similar VDF are shown below. Again, the following simplifying terms are defined for brevity as:

$$u_j = V_j - v_{oj} \tag{A25a}$$

$$w_j = \frac{u_j}{V_{Tj}} \tag{A25b}$$

$$\psi\left(z\right) = \frac{\Gamma'\left(z\right)}{\Gamma\left(z\right)} \equiv \text{digamma function} \tag{A25c}$$

where $\Gamma(z)$ is the Riemann gamma function of argument z. After denoting the VDF in Equation A20 as $f^{(ss)}$, the partial derivatives are given by:

$$\frac{\partial f^{(ss)}}{\partial n_o} = \frac{f^{(ss)}}{n_o} \tag{A26a}$$
$$\frac{\partial f^{(ss)}}{\partial V_{T\parallel}} = \left(\frac{s \ w_{\parallel}{}^{s} - 1}{V_{T\parallel}} \right) \ f^{(ss)} \tag{A26b}$$
$$\frac{\partial f^{(ss)}}{\partial V_{T\perp}} = \left(\frac{s \ w_{\perp}{}^{s} - 2}{V_{T\perp}} \right) \ f^{(ss)} \tag{A26c}$$
$$\frac{\partial f^{(ss)}}{\partial v_{o\parallel}} = \left(\frac{s \ w_{\parallel}{}^{s-1}}{V_{T\parallel}} \right) \ f^{(ss)} \tag{A26d}$$
$$\frac{\partial f^{(ss)}}{\partial v_{o\perp}} = \left(\frac{s \ w_{\perp}{}^{s-1}}{V_{T\perp}} \right) \ f^{(ss)} \tag{A26e}$$
$$\frac{\partial f^{(ss)}}{\partial s} = \left[\frac{3 \ \psi\left(\frac{1+s}{s}\right)}{s^2} - w_{\parallel}{}^{s} \ \ln w_{\parallel} - w_{\perp}{}^{s} \ \ln w_{\perp} \right] \ f^{(ss)} \tag{A26f}$$

After denoting the VDF in Equation A24b as $f^{(as)}$, the partial derivatives are given by:

$$\frac{1}{f^{(as)}} \frac{\partial f^{(as)}}{\partial n_o} = \frac{1}{n_o} \tag{A27a}$$
$$\frac{1}{f^{(as)}} \frac{\partial f^{(as)}}{\partial V_{T\parallel}} = \left(\frac{p \ w_{\parallel}{}^{p} - 1}{V_{T\parallel}} \right) \tag{A27b}$$
$$\frac{1}{f^{(as)}} \frac{\partial f^{(as)}}{\partial V_{T\perp}} = \left(\frac{q \ w_{\perp}{}^{q} - 2}{V_{T\perp}} \right) \tag{A27c}$$
$$\frac{1}{f^{(as)}} \frac{\partial f^{(as)}}{\partial v_{o\parallel}} = \left(\frac{p \ w_{\parallel}{}^{p-1}}{V_{T\parallel}} \right) \tag{A27d}$$
$$\frac{1}{f^{(as)}} \frac{\partial f^{(as)}}{\partial v_{o\perp}} = \left(\frac{q \ w_{\perp}{}^{q-1}}{V_{T\perp}} \right) \tag{A27e}$$
$$\frac{1}{f^{(as)}} \frac{\partial f^{(as)}}{\partial p} = \frac{\psi\left(\frac{1+p}{p}\right)}{p^2} - w_{\parallel}{}^{p} \ \ln w_{\parallel} \tag{A27f}$$
$$\frac{1}{f^{(as)}} \frac{\partial f^{(as)}}{\partial q} = \frac{2 \ \psi\left(\frac{1+q}{q}\right)}{q^2} - w_{\perp}{}^{q} \ \ln w_{\perp} \tag{A27g}$$

Acknowledgements

The authors thank A.F.- Viñas, B. Lembège, and D.A. Roberts for useful discussions of collisionless shock physics. The authors thank the Harvard Smithsonian Center for Astrophysics, the Space Science Laboratory at Berkeley, and the NASA SPDF/CDAWeb team for the interplanetary shock analysis and *Wind* data.

REFERENCES

Abraham-Shrauner, B., & Yun, S. H. 1976, J. Geophys. Res., 81, 2097, doi: 10.1029/JA081i013p02097

Dum, C. T. 1975, Phys. Rev. Lett., 35, 947, doi: 10.1103/PhysRevLett.35.947

Dum, C. T., Chodura, R., & Biskamp, D. 1974, Phys. Rev. Lett., 32, 1231, doi: 10.1103/PhysRevLett.32.1231

Edmiston, J. P., & Kennel, C. F. 1984, J. Plasma Phys., 32, 429

Feldman, W. C., Anderson, R. C., Bame, S. J., et al. 1983a, J. Geophys. Res., 88, 9949, doi: 10.1029/JA088iA12p09949

Feldman, W. C., Asbridge, J. R., Bame, S. J., & Gosling, J. T. 1979a, J. Geophys. Res., 84, 7371, doi: 10.1029/JA084iA12p07371

Feldman, W. C., Asbridge, J. R., Bame, S. J., Gosling, J. T., & Lemons, D. S. 1979b, J. Geophys. Res., 84, 4463, doi: 10.1029/JA084iA08p04463

Feldman, W. C., Anderson, R. C., Bame, S. J., et al. 1983b, J. Geophys. Res., 88, 96, doi: 10.1029/JA088iA01p00096

Goldman, M. V. 1984, Rev. Modern Phys., 56, 709, doi: 10.1103/RevModPhys.56.709

Horton, W., & Choi, D. 1979, Phys. Rep., 49, 273, doi: 10.1016/0370-1573(79)90056-5

Horton, Jr., W., Choi, D.-I., & Koch, R. A. 1976, Phys. Rev. A, 14, 424, doi: 10.1103/PhysRevA.14.424

Jain, H. C., & Sharma, S. R. 1979, Beitraege Plasmaphysik, 19, 19

Kasper, J. C., Lazarus, A. J., Steinberg, J. T., Ogilvie, K. W., & Szabo, A. 2006, J. Geophys. Res., 111, 3105, doi: 10.1029/2005JA011442

Kennel, C. F., Edmiston, J. P., & Hada, T. 1985, in Geophys. Monogr. Ser., Vol. 34, Collisionless Shocks in the Heliosphere: A Tutorial Review, ed. R. G. Stone & B. T. Tsurutani (Washington, D.C.: AGU), 1–36

Koval, A., & Szabo, A. 2008, J. Geophys. Res., 113, 10110, doi: 10.1029/2008JA013337

Krall, N. A., & Trivelpiece, A. W. 1973, Principles of plasma physics

Krasnoselskikh, V. V., Lembège, B., Savoini, P., & Lobzin, V. V. 2002, Phys. Plasmas, 9, 1192, doi: 10.1063/1.1457465

Lazar, M., Fichtner, H., & Yoon, P. H. 2016, Astron. & Astrophys., 589, A39, doi: 10.1051/0004-6361/201527593

Lazar, M., Pierrard, V., Shaaban, S. M., Fichtner, H., & Poedts, S. 2017, Astron. & Astrophys., 602, A44, doi: 10.1051/0004-6361/201630194

Lazar, M., Poedts, S., & Fichtner, H. 2015a, Astron. & Astrophys., 582, A124, doi: 10.1051/0004-6361/201526509

Lazar, M., Poedts, S., Schlickeiser, R., & Dumitrache, C. 2015b, Mon. Not. Roy. Astron. Soc., 446, 3022, doi: 10.1093/mnras/stu2312

Lazar, M., Shaaban, S. M., Fichtner, H., & Poedts, S. 2018, Phys. Plasmas, 25, 022902, doi: 10.1063/1.5016261

Lepping, R. P., Acũna, M. H., Burlaga, L. F., et al. 1995, Space Sci. Rev., 71, 207, doi: 10.1007/BF00751330

Livadiotis, G. 2015, J. Geophys. Res., 120, 1607, doi: 10.1002/2014JA020825

Livadiotis, G., Desai, M. I., & Wilson III, L. B. 2018, Astrophys. J., 853, 15, doi: 10.3847/1538-4357/aaa713

Mace, R. L., & Sydora, R. D. 2010, J. Geophys. Res., 115, 7206, doi: 10.1029/2009JA015064

Maksimovic, M., Pierrard, V., & Riley, P. 1997, Geophys. Res. Lett., 24, 1151, doi: 10.1029/97GL00992

Markwardt, C. B. 2009, in Astronomical Society of the Pacific Conference Series, Vol. 411, Astronomical Data Analysis Software and Systems XVIII, ed. D. A. Bohlender, D. Durand, & P. Dowler, 251

Matyka, M., Gołembiewski, J., & Koza, Z. 2016, Phys. Rev. E, 93, 013110, doi: 10.1103/PhysRevE.93.013110

Ogilvie, K. W., Chornay, D. J., Fritzenreiter, R. J., et al. 1995, Space Sci. Rev., 71, 55, doi: 10.1007/BF00751326

Pulupa, M. P., Salem, C., Phan, T. D., Gosling, J. T., & Bale, S. D. 2014, Astrophys. J. Lett., 791, L17, doi: 10.1088/2041-8205/791/1/L17

Russell, C. T., Gosling, J. T., Zwickl, R. D., & Smith, E. J. 1983, J. Geophys. Res., 88, 9941, doi: 10.1029/JA088iA12p09941

Saeed, S., Sarfraz, M., Yoon, P. H., Lazar, M., & Qureshi, M. N. S. 2017, Mon. Not. Roy. Astron. Soc., 465, 1672, doi: 10.1093/mnras/stw2900

Salem, C., Hubert, D., Lacombe, C., et al. 2003, Astrophys. J., 585, 1147, doi: 10.1086/346185

Shaaban, S. M., Lazar, M., & Poedts, S. 2018, Mon. Not. Roy. Astron. Soc., 480, 310, doi: 10.1093/mnras/sty1567

Szabo, A. 1994, J. Geophys. Res., 99, 14737, doi: 10.1029/94JA00782

Vasyliunas, V. M. 1968, J. Geophys. Res., 73, 2839, doi: 10.1029/JA073i009p02839

Vinas, A. F., & Scudder, J. D. 1986, J. Geophys. Res., 91, 39, doi: 10.1029/JA091iA01p00039